Desalination and Water Treatment
www.deswater.com

doi: 10.1080/19443994.2016.1157045

57 (2016) 29212–29219
December

Taylor & Francis
Taylor & Francis Group

Kinetics of hydroquinone oxidation by a wire–cylinder dielectric barrier discharge reactor

Wei Wang[a,*], Shun Wang[a], Jingwei Feng[a], Shoujun Yuan[a], Zhenhu Hu[a,*], Julian Muñoz Sierra[b], Xuedong Zhang[b]

[a]*Department of Municipal Engineering, School of Civil and Hydraulic Engineering, Hefei University of Technology, Hefei 230009, China, Tel. +86 13655605619; emails: dwhit@126.com (W. Wang), 767073806@qq.com (S. Wang), fengjingwei200@163.com (J. Feng), yuanshoujun1976@163.com (S. Yuan), zhhu@hfut.edu.cn (Z. Hu)*

[b]*Section Sanitary Engineering, Department of Water Management, Delft University of Technology, Delft 2828CN, The Netherlands, emails: J.D.MunozSierra@tudelft.nl (J. Muñoz Sierra), X.Zhang@tudelft.nl (X. Zhang)*

Received 7 November 2015; Accepted 27 January 2016

ABSTRACT

The effects of discharge power, voltage/current, initial concentration, pH, and air flow rate on the oxidative degradation of hydroquinone were investigated, respectively, by a wire–cylinder dielectric barrier discharge reactor under a NaCl concentration of 10 g/L. Results indicated that the removal efficiency of hydroquinone increased from 74.6 to 88.2% when the discharge power increased from 30 to 50 W. Moreover, an enhancement from 68.5 to 85.6% was observed when the air flow rate changed from 20 to 40 L/h, at 10-min reaction time and an initial hydroquinone concentration of 40 mg/L. The observed maximum pseudo-first-order kinetic constant was about $0.3820 \pm 0.0409\ \text{min}^{-1}$ under a discharge power of 60 W and air flow rate of 80 L/h. Compared with other factors, discharge power, pH, and air flow rate played a significant role in improving the oxidation rates of hydroquinone. This work provides new insights into our understanding of plasma-induced degradation of hydroquinone under a NaCl concentration of 10 g/L.

Keywords: Hydroquinone; Plasma; Wire–cylinder dielectric barrier discharge reactor; Oxidative degradation; Catalytic effect

1. Introduction

Phenolic compounds widely used as biocides, pesticides, and preservatives have been broadly found in industrial effluents, such as coal gasification wastewater, coking wastewater, olive mill wastewater among others [1]. Due to their toxicity and resistance, biological treatment of phenolic compounds still faces major challenges. Previous studies indicated the existence of low concentrations of phenols and its degradation intermediates in the biological effluent [2,3]. Hydroquinone appears to be one of the main toxic metabolites from phenols and benzene, which often leads to potential threats in the aquatic environment. Thus, it is an unavoidable pollutant to deal with when

---

*Corresponding authors.

Presented at the 8th International Conference on Challenges in Environmental Science & Engineering (CESE-2015)
28 September–2 October 2015, Sydney, Australia

the wastewaters containing phenolic and benzene compounds are treated.

Advanced oxidation processes (AOPs), e.g. ozonation, photocatalysis, and Fenton oxidation, have been applied for the advanced treatment of phenolic wastewaters. Esplugas et al. studied AOPs for phenol degradation including ozone and its combination, photolysis and UV/H_2O_2, Fenton reagent and photocatalysis [4]. The pseudo-first-order kinetic models fitted the experimental data well and the maximum value of pseudo-first-order kinetic constant reached 22.2 h^{-1} within the Fenton oxidation. Wang et al. used a synthesized Fe_3O_4/CS supported on Co_3O_4 nanoparticles to oxidize phenol and almost achieved complete degradation within 30 min [5]. Evidently, the application of AOPs led to attain high degradation rates of phenolic pollutants when the biological treatment did not achieve its maximum bioconversion capacity. However, it should be pointed out that the AOPs still relied on the high cost of reagents such as hydrogen peroxide, ozone, or low-energy-intensive technologies.

Hydroquinone is identified as the intermediate of the oxidation degradation of phenolic compounds. It is not easy to be degraded and not economically feasible to be mineralized using the conventional AOPs. Plasma technology is characterized by a high energy-intensive demand (however, non-thermal plasma uses less energy consumption and offers a higher selectivity than thermal plasma chemical reactions), effective oxidation and a minimized production of byproducts. Strongly oxidative species such as $\cdot OH$, $\cdot O$, $\cdot HO_2$, H_2O_2, O_3 are generated in the gas–liquid interface to initiate chemical reactions making a feasible treatment of hydroquinone become possible. Previous studies also indicated such oxidative species for phenol degradation were obtained in plasma and plasma–photocatalysis systems [6,7]. Since applying wire–cylinder dielectric barrier discharge reactor technology provided a considerable reduction of energy consumption and an increase in efficiency [8], its use to enhance the degradation rate of hydroquinone in the aquatic environment was implemented.

The aim of this paper is to analyze the effects of different parameters, i.e. discharge power, voltage/current, initial concentration, pH, and air flow rate on the oxidative degradation of hydroquinone by a wire–cylinder dielectric barrier discharge reactor under a NaCl concentration of 10 g/L. The pseudo-first- and pseudo-second-order kinetic models are compared by describing hydroquinone oxidation rates and reaction time values.

2. Materials and methods

2.1. Experimental setup

The schematic diagram of wire–cylinder dielectric barrier discharge reactor is shown in Fig. 1. The system included a high-frequency high-voltage power source (CTP-2000 K, Nanjing Suman Electronics Co., Ltd, China), an air pump, and a dielectric barrier discharge reactor. The dielectric barrier discharge reactor was made of the organic glass cylinder (50 mm inner diameter and 80 mm outer diameter). A quartz tube (15 mm in diameter, 250 mm in length) with a copper rod as the discharge electrode was installed in the middle of the reactor, and the negative electrode was set at the bottom of reactor. The air was supplied by an electromagnetic air pump (ACO-004, Zhejiang sensen industrial Co., Ltd, China), and the flow rate was controlled by a gas meter (LZB-4, shanghai splendor instrument and meter plant, China). The temperature of the reactor was controlled by a cold water jacket.

2.2. Experimental procedure

The effects of discharge power, voltage/current, initial concentration, pH, and air flow rate on the oxidative degradation of hydroquinone were studied in the wire–cylinder dielectric barrier discharge reactor under a NaCl concentration of 10 g/L. The volume of hydroquinone solution was 200 mL and the pH of the solution was adjusted by 0.1 mol/L NaOH and 0.1 mol/L HCl. The experimental procedure and conditions applied are shown in Table 1. All the tests were performed in duplicates.

2.3. Analytical methods

The pH and temperature were monitored by a pH meter (SG23-SevenGo Duo, Mettler-Toledo). The concentration of hydroquinone was analyzed using high-performance liquid chromatography (HPLC, 1260 Infinity, Agilent, USA) with a C_{18} column (Inertsil ODS-3, 4.6 × 250 mm, 5 μm, GL Sciences Inc., Japan). The HPLC system was maintained at 30°C. The injection volume was 20 μL and the detection wavelength of UV detector was 280 nm. The mobile phase used was acetonitrile and water (25:75, v/v), and the flow rate was 1.0 mL/min.

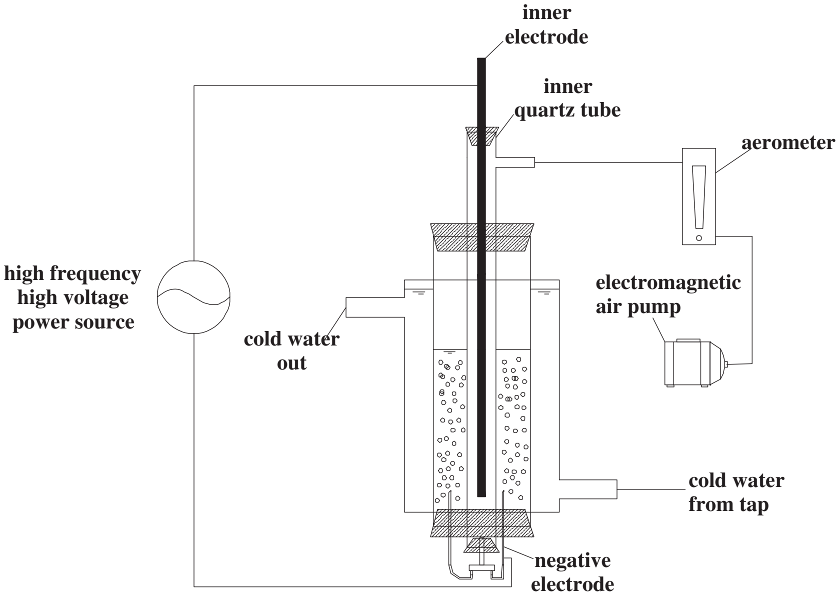

Fig. 1. Schematic diagram of wire–cylinder dielectric barrier discharge reactor.

Table 1
Parameters and different conditions applied of the experiments

No.	Power (W)	Voltage/Current (V/A)	Initial pH	Air flow rate (L/h)	Hydroquinone (mg/L)
1	60	100/0.6	Uncontrolled (pH 5–6)	40	100
	50	100/0.5			
	40	100/0.4			
	30	100/0.3			
2	60	100/0.6			20
					40
					60
3	60	120/0.5			40
		75/0.8			
		150/0.4			
4	60	100/0.6	3		40
			7		
			9		
5	60	100/0.6	Uncontrolled (pH 5–6)	20	40
				80	

3. Results and discussion

3.1. Effect of discharge power on the degradation of hydroquinone and changes of reaction ($t_{1/2}$ and $t_{3/4}$) time under a NaCl concentration of 10 g/L

The degradation of hydroquinone and changes of reaction time ($t_{1/2}$ and $t_{3/4}$) under high salinity condition are shown in Fig. 2. The values of $t_{1/2}$ and $t_{3/4}$ represent the reaction time when the hydroquinone reductions reach to 50–75%, respectively. It could be observed that in the first 10 min the best results were obtained when a discharge power of 50 W was applied because the contribution of the amount of active species increased while more power was applied. The minimum and maximum removal rates of hydroquinone were 74.6–88.2% at powers of 30–50 W, respectively. Subsequently, the results of all groups reached above 97% removal of hydroquinone after 50 min oxidation. The reaction time values exhibited that the shortest $t_{1/2}$ and $t_{3/4}$ were 3.07 min at a power of 60 W and 5.83 min at a power of 50 W, correspondingly.

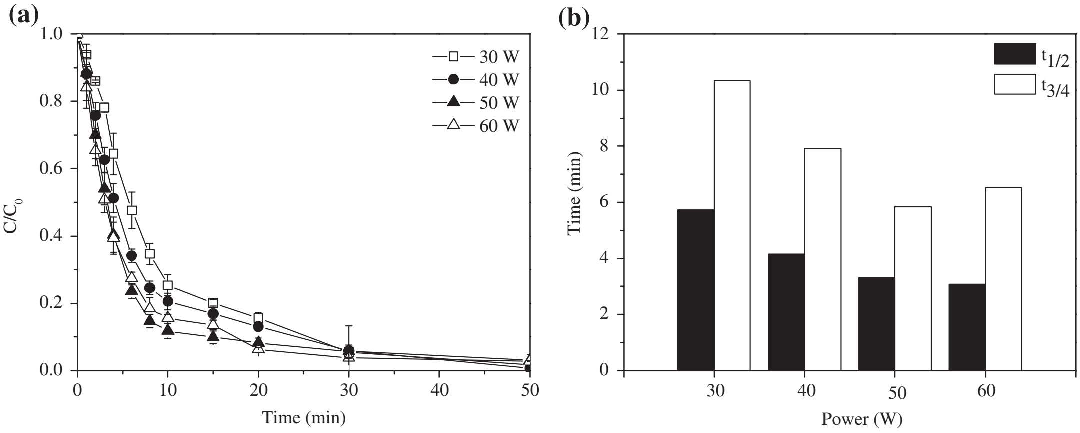

Fig. 2. (a) Effect of discharge power on the degradation of hydroquinone and (b) Changes of reaction time ($t_{1/2}$ and $t_{3/4}$) under a NaCl concentration of 10 g/L.

According to the values of reaction time $t_{1/2}$, the degradation rates of hydroquinone were enhanced by the increasing discharge power during the earlier reaction period. As the values of $t_{1/2}$ were approximately equal to the half of the reaction time $t_{3/4}$ in most of the cases, it was possible to postulate that reactions followed a first-order kinetic model. The pseudo-first-order kinetic model well fitted the experimental data during the first 10 min with values higher than 0.99 from the coefficient of determination R^2, as shown in Table 2. The highest kinetic constant was around 0.2671 min^{-1} at power of 50 W instead of 60 W, 1.78 times higher than the constant at a power of 30 W. During the experiments, the pH value decreased dramatically in the aqueous solution because of the protons production within the degradation reaction of hydroquinone (Eq. (1)). After the reaction time $t_{1/2}$, the pH values at a power of 60 W were lower than the values at a power of 50 W, and both of them decreased to below 3.5. Previous studies indicated that hydrogen ion acts as ·OH radical scavengers at very low pH values [9]. This might be the reason for the decrease in the degradation kinetic constants of hydroquinone at a power of 60 W. Similar trend was also reported for the degradation of phenol by an electrochemical oxidation process [10].

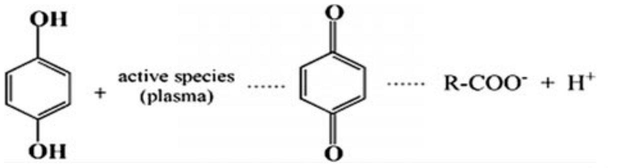

(1)

3.2. Effect of initial concentrations on degradation of hydroquinone and kinetic constants under a NaCl concentration of 10 g/L

Fig. 3 shows the effect of initial concentrations on the degradation of hydroquinone and the changes of reaction time ($t_{1/2}$ and $t_{3/4}$) under a NaCl concentration of 10 g/L. The concentration of hydroquinone decreased to 1.73, 4.43, 7.84, and 14.83 mg/L during the first 10 min from an initial concentration of 20, 40,

Table 2
Analysis of pseudo-first- and pseudo-second-order kinetics at different applied power under a NaCl concentration of 10 g/L

	Pseudo-first-order kinetic				Pseudo-second-order kinetic	
	0–$t_{3/4}$ min		$t_{3/4}$–50 min		0–50 min	
Power (W)	K_1 (min^{-1})	R^2	K_2 (min^{-1})	R^2	K (L/mg min^{-1})	R^2
30	0.1504 ± 0.0153	0.9926	0.0750 ± 0.0247	0.9686	0.0036 ± 0.0004	0.9849
40	0.1873 ± 0.0056	0.9979	0.0873 ± 0.0019	0.9769	0.0055 ± 0.0001	0.9381
50	0.2671 ± 0.0010	0.9985	0.0376 ± 0.0103	0.9841	0.0079 ± 0.0035	0.9717
60	0.2160 ± 0.0118	0.9934	0.0448 ± 0.0031	0.8528	0.0082 ± 0.0004	0.9744

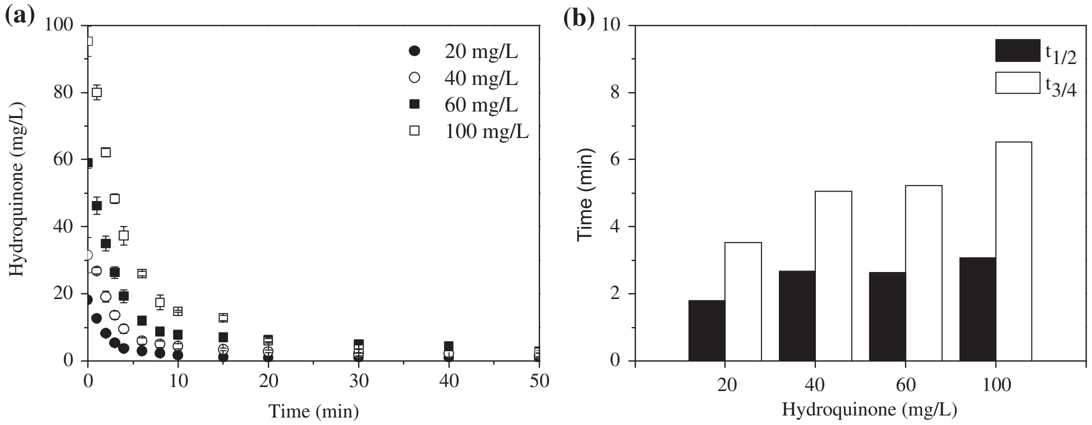

Fig. 3. (a) Effect of initial concentrations on degradation of hydroquinone and (b) Changes of reaction time ($t_{1/2}$ and $t_{3/4}$) under a NaCl concentration of 10 g/L.

60, and 100 mg/L, respectively. Accordingly, the removal efficiencies achieved were of 90.6, 86.0, 86.7, and 84.4%. Correspondingly, the final concentrations of hydroquinone observed were 0.96, 1.73, 3.04, and 2.59 mg/L after 50 min reaction. As can be observed from Fig. 3(b), the reaction time $t_{1/2}$ and $t_{3/4}$ of hydroquinone degradation with an initial concentration of 100 mg/L were 1.70–1.85 times longer than with an initial concentration of 20 mg/L. This result was attributed to the impact on the removal rate of hydroquinone due to its initial concentration. The specific degradation rates decreased with a higher initial concentration exhibiting a negative correlation between them, more likely due to a lack of active species supply [11].

The kinetic constants (0–$t_{3/4}$ min) in Table 3 can illustrate the experimental data fitting (all of R^2 values are higher than 0.99) to a pseudo-first-order model. It was imperative to mention that there was a turning point in kinetic constants after a reaction time of $t_{3/4}$ in almost all of the cases tested. The kinetic constants ($t_{3/4\text{–}50}$ min) were only 1/5–1/20 of the kinetic constants observed at 0–$t_{3/4}$ min. This led to two different explanations. On the one hand, it was difficult to achieve complete mineralization of hydroquinone by plasma and the accumulation of byproducts made the degradation rates significantly slow down. On the other hand, the declining pH led to a decrease in the oxidation efficiency of hydroquinone. The use of plasma could not be efficient and most probably not economically suitable to achieve complete mineralization of hydroquinone under the conditions applied. Therefore, shortening the reaction time to enhance the oxidation process of hydroquinone was required and important for further development of applying plasma reactor technology.

3.3. *Effect of voltage/current on the kinetic constants of hydroquinone and changes of reaction time ($t_{1/2}$ and $t_{3/4}$) under a NaCl concentration of 10 g/L*

In order to examine the effects of voltage and current on the degradation of hydroquinone, four different voltages and currents were setup under a

Table 3
Analysis of pseudo-first- and pseudo-second-order kinetic for different initial concentration of hydroquinone under a NaCl concentration of 10 g/L

	Pseudo-first-order kinetic				Pseudo-second-order kinetic	
	0–$t_{3/4}$ min		$t_{3/4}$–50 min		0–50 min	
Concentration (mg/L)	K_1 (min^{-1})	R^2	K_2 (min^{-1})	R^2	K (L/mg min^{-1})	R^2
20	0.4055 ± 0.0092	0.9981	0.0199 ± 0.0048	0.5922	0.0215 ± 0.0045	0.7603
40	0.3041 ± 0.0237	0.9909	0.0262 ± 0.0049	0.8898	0.0123 ± 0.0044	0.9371
60	0.2733 ± 0.0070	0.9975	0.0232 ± 0.0006	0.9834	0.0056 ± 0.0006	0.9430
100	0.2160 ± 0.0118	0.9934	0.0448 ± 0.0031	0.8528	0.0082 ± 0.0004	0.9744

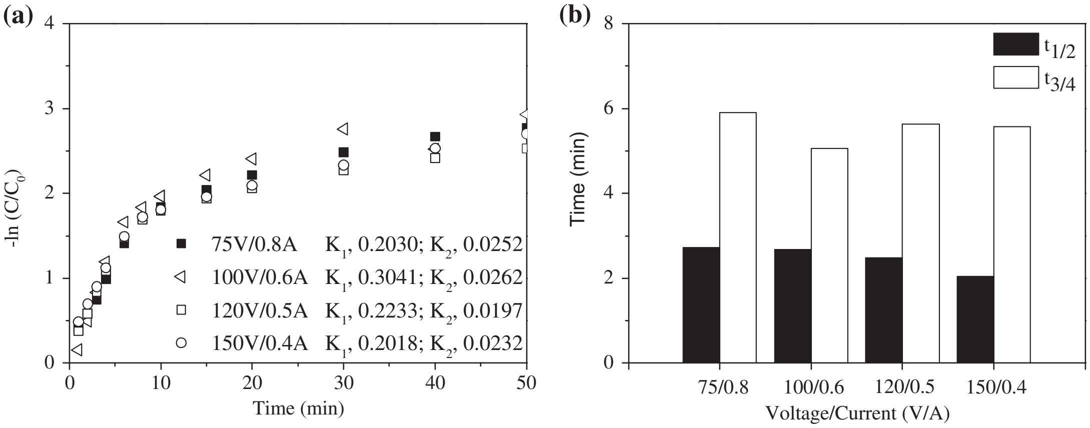

Fig. 4. (a) Effect of voltage/current on the kinetic constants of hydroquinone and (b) Changes of reaction time ($t_{1/2}$ and $t_{3/4}$) under a NaCl concentration of 10 g/L.

fixed discharge power of 60 W. The influence of voltage/current on kinetic constants of hydroquinone and changes of reaction time ($t_{1/2}$ and $t_{3/4}$) are shown in the Fig. 4. As compared to other factors, the changes of voltage and current did not bring apparently impact on the degradation of hydroquinone under the same power condition. At $t_{3/4}$, the first-order kinetic constants were around 0.2018–0.3041 min^{-1}. The maximum constant of 0.3041 min^{-1} was obtained at a voltage/current of 100 V/0.6A. The shortest $t_{1/2}$ and $t_{3/4}$ were 2.0–5.0 min at voltage/current of 150–100 V/0.6A, respectively, but there were no significant differences among them. The removal efficiencies of hydroquinone achieved were about 92–94.3% after 50 min reaction. Previous studies indicated that the application of a higher voltage promoted the production of ozone (O_3), and the generation of hydrogen peroxide H_2O_2 had a close relation with current while the conductivity was fixed [12]. Nevertheless, the total amount of active species (O_3, $OH^{\cdot}$ and H_2O_2) might be similar, while the same discharge intensity was applied [13]. Consequently, there would be some differences in the degradation rates of hydroquinone in a short time, but overall the degradation rates were similar to each other. This was in accordance with the experimental results observed in the current study.

3.4. Effect of initial pH on degradation of hydroquinone and kinetic constants under a NaCl concentration of 10 g/L

The effect of initial pH on the degradation of hydroquinone and the kinetic constants are shown in Fig. 5. The results showed that removal efficiency of hydroquinone could reach a maximum value of 94.3% with an initial pH of 5. Other removal efficiencies after 50 min oxidation were observed about 89.2, 88.3, and 90.6% at pH levels of 3, 7, and 9, respectively. In addition, the largest values for the kinetic constants K_1 and K_2 of about 0.3041 and 0.0262 min^{-1} were also obtained at the initial pH of 5. This condition might generate a higher amount of radicals $^{\cdot}OH$ being more active than H_2O_2 under an initial pH value of 5. Whereas the pH was around high values, the $^{\cdot}OH$ was also scavenged with the decomposing of $HO_2^{\cdot}$ ion [14]. It must be pointed out the shortest reaction times ($t_{1/2}$ and $t_{3/4}$) of 0.7–4.2 min, respectively, were obtained at an initial pH of 9, exceeding the values of 2.7–5.0 min correspondingly with an initial pH of 5. In the first step of the oxidation, hydroquinone must be deprotonated in terms of the electrochemistry evidence of quinine and the activation barrier of hydroquinone oxidation [15]. With an increase in pH above 7.0, the mono-dissociated and doubled-dissociated anions of hydroquinone could be generated, being more readily oxidized than hydroquinone [16]. However, after a reaction time of 1 min took place, the solution pH decreased from 9 to below than 4 with a hydroquinone removal of 68% (Eq. (2)). Because of the low pH and accumulation of byproducts, the degradation rate of hydroquinone subsequently exhibited a significant decrease. This outcome could explain the reason why the shortest reaction time was achieved at an initial pH of 9 while the constant K_1 was not the largest.

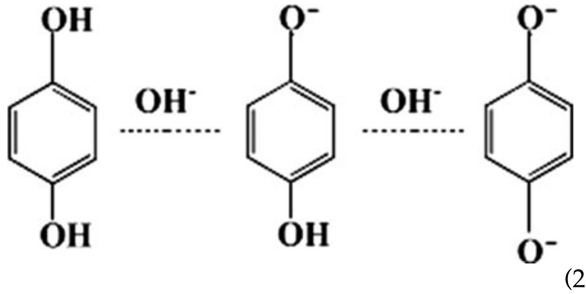

(2)

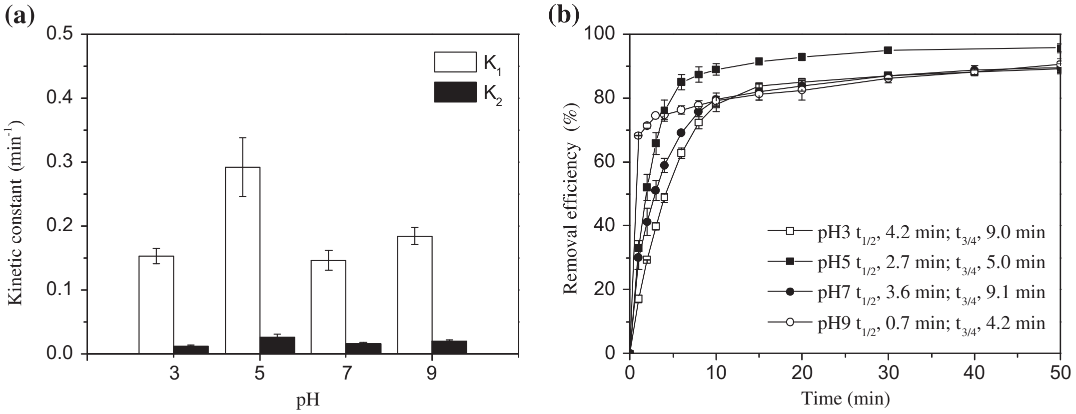

Fig. 5. (a) Effect of initial pH on the degradation of hydroquinone and (b) The kinetic constants under a NaCl concentration of 10 g/L.

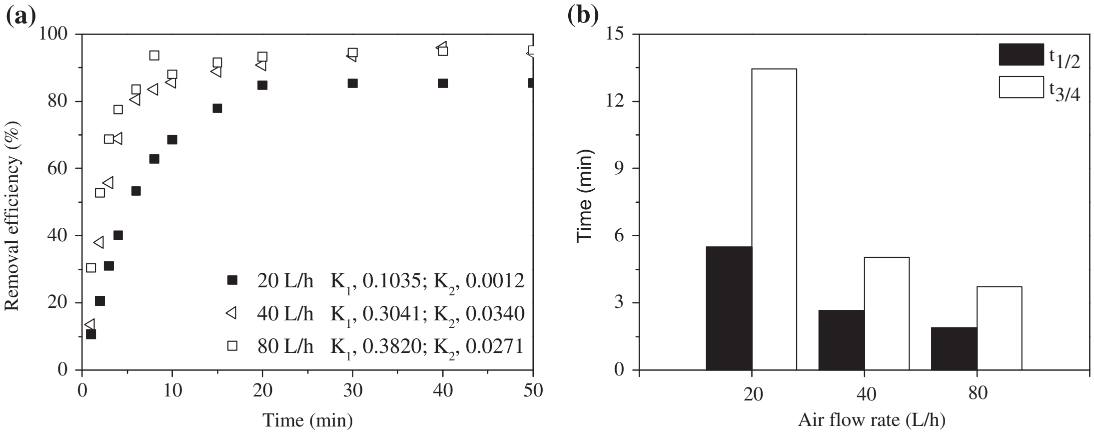

Fig. 6. (a) Effect of air flow rates on degradation of hydroquinone and (b) Changes of reaction time ($t_{1/2}$ and $t_{3/4}$) under a NaCl concentration of 10 g/L.

3.5. Effect of air flow rates on the degradation of hydroquinone and changes of reaction time ($t_{1/2}$ and $t_{3/4}$) under a NaCl concentration of 10 g/L

The impact of air flow rate was evaluated since the active species, such as $OH^{\cdot}$ and O_3 could be generated in the interface of gas–liquid, and the oxidative reagents could diffuse into the water to react with the target molecules [17], in this case influencing the degradation of hydroquinone in the dielectric barrier discharge reactor system. The results (Fig. 6) indicated an increasing conversion of hydroquinone while the air flow rates were increased. The first-order kinetic constant K_1 changed from 0.1035 to 0.3041 min^{-1} by doubling the air flow rate from 20 to 40 L/h. Also, the reaction time of $t_{1/2}$ and $t_{3/4}$ shortened from 5.5–13.4 to 2.7–5.0 min, respectively. However, when the air flow rate was further increased to 80 L/h, the improvement was negligible. The reason might be that the interface of gas–liquid was already saturated with oxygen, and the active species were blown away by the excessive air flow before they reacted with hydroquinone [18]. Therefore, an optimization of the air flow rate was necessary to achieve a maximized combination of diffusion and reaction from the active species.

4. Conclusions

The discharge power, pH, and air flow rate played an important role on the oxidative degradation of hydroquinone in the wire–cylinder dielectric barrier discharge reactor under a NaCl concentration of 10 g/L. The basic pH condition might benefit the initial conversion of hydroquinone in the reaction time

$t_{1/2}$, but the degradation rate of hydroquinone depended critically on the air flow rate in the reaction time $t_{3/4}$. The pseudo-first-order kinetic models well fitted the oxidation rate of hydroquinone in the reaction time $t_{1/2}$. The plasma technology provides a potential way to enhance the degradation of hydroquinone in the aquatic environment, but the optimum conditions still need to be explored.

Acknowledgments

This work was supported by the National Natural Science Foundation of China (No. 51208164) and China Scholarship Council (No. 201406695003).

References

[1] W. Wang, J. Zhang, S. Wang, J. Shen, Oxygen-limited aeration for relieving the impact of phenolic compounds in anaerobic treatment of coal gasification wastewater, Int. Biodeterior. Biodegrad. 95 (2014) 110–116.

[2] W. Wang, H.J. Han, Recovery strategies for tackling the impact of phenolic compounds in a UASB reactor treating coal gasification wastewater, Bioresour. Technol. 103 (2012) 95–100.

[3] W. Wang, S.L. Pan, R.J. Xu, J. Zhang, S. Wang, J. Shen, Competitive adsorption behaviors, characteristics, and dynamics of phenol, cresols, and dihydric phenols onto granular activated carbon, Desalin. Water Treat. 56 (2015) 770–778.

[4] S. Esplugas, J. Giménez, S. Contreras, E. Pascual, M. Rodríguez, Comparison of different advanced oxidation processes for phenol degradation, Water Res. 36 (2002) 1034–1042.

[5] Y.X. Wang, H.Q. Sun, H.M. Ang, M.O. Tadé, S.B. Wang, Magnetic Fe_3O_4/carbon sphere/cobalt composites for catalytic oxidation of phenol solutions with sulfate radicals, Chem. Eng. J. 245 (2014) 1–9.

[6] H.J. Wang, X.Y. Chen, Kinetic analysis and energy efficiency of phenol degradation in a plasma-photocatalysis system, J. Hazard. Mater. 186 (2011) 1888–1892.

[7] H.J. Wang, J. Li, X. Quan, Y. Wu, Enhanced generation of oxidative species and phenol degradation in a discharge plasma system coupled with TiO_2 photocatalysis, Appl. Catal. B 83 (2008) 72–77.

[8] S.F. Tang, N. Lu, J. Li, K.F. Shang, Y. Wu, Improved phenol decomposition and simultaneous regeneration of granular activated carbon by the addition of a titanium dioxide catalyst under a dielectric barrier discharge plasma, Carbon 53 (2013) 380–390.

[9] X.R. Xu, X.Y. Li, X.Z. Li, H.B. Li, Degradation of melatonin by UV, UV/H_2O_2, Fe^{2+}/H_2O_2 and UV/Fe^{2+}/H_2O_2 processes, Sep. Purif. Technol. 68 (2009) 261–266.

[10] Z.C. Wu, M.H. Zhou, Partial degradation of phenol by advanced electrochemical oxidation process, Environ. Sci. Technol. 35 (2001) 2698–2703.

[11] D. He, Y.B. Sun, L. Xin, J.W. Feng, Aqueous tetracycline degradation by non-thermal plasma combined with nano-TiO_2, Chem. Eng. J. 258 (2014) 18–25.

[12] M. Sato, T. Ohgiyama, J.S. Clements, Formation of chemical species and their effects on microorganisms using a pulsed high-voltage discharge in water, IEEE Trans. Ind. Appl. 32 (1996) 106–112.

[13] J. Li, M. Sato, T. Ohshima, Degradation of phenol in water using a gas–liquid phase pulsed discharge plasma reactor, Thin Solid Films 515 (2007) 4283–4288.

[14] J.B. Zhang, Z. Zheng, Y.N. Zhang, J.W. Feng, J.H. Li, Low-temperature plasma-induced degradation of aqueous 2,4-dinitrophenol, J. Hazard. Mater. 154 (2008) 506–512.

[15] T.A. Link, The role of the 'Rieske' iron sulfur protein in the hydroquinone oxidation (QP) site of the cytochrome bc1 complex: The 'proton-gated affinity change' mechanism, FEBS Lett. 412 (1997) 257–264.

[16] X. Yuan, A.N. Pham, C.J. Miller, T.D. Waite, Copper-catalyzed hydroquinone oxidation and associated redox cycling of copper under conditions typical of natural saline waters, Environ. Sci. Technol. 47 (2013) 8355–8364.

[17] D.X. Jiang, X.H. Zheng, H.H. Xu, N.B. Wong, X-ray diffraction, DFT, spectroscopic study and insecticidal activity of (3-cyano-1-(2,6-dichloro-4-(trifluoromethyl) phenyl)-4-((trifluoromethyl)sulfinyl)-1H-pyrazol-5-yl) (2-(triethylammonio)acetyl)amide inner salt, Crystallogr. Rep. 59 (2014) 1078–1083.

[18] C. Geng, C.D. Wu, H.J. Wang, C.W. Yi, Effect of chemical parameters on pyrene degradation in soil in a pulsed discharge plasma system, J. Electrostat. 73 (2015) 38–42.